# INFLUENCE OF THE ACOUSTIC ENTRAINMENT ON AEROSOL PARTICLE INTERACTIONS: EXPERIMENTAL BALANCE OF THE HYDRODYNAMIC MECHANISMS

PACS REFERENCE:43.25.Uv, 43.25.Nm

González Icíar: Gallego Juan A.; Riera Enrique
Instituto de Acústica, CSIC
Calle Serrano 144
28006 Madrid
Spain
Tel: 34915618806
Fax: 34914117651
iacgg38@ia.cetef.csic.es

**ABSTRACT**

A new experimental micro-scale study of particle interactions acoustically induced in monodisperse aerosols is presented in this work. It is devoted to the study of the influence exerted by the acoustic entrainment experienced by the single particles on their attraction processes and, in particular, on the hydrodynamic mechanisms that govern them. Glass spheres with certified diameters of $8.0 \pm 0.9 mm$ immersed in air as dilute aerosols were subjected to homogeneous plane standing waves with a constant velocity amplitude $U_0$=0.44m/s at diverse frequencies, ranging from 200Hz up to 5kHz, at which the particles were much smaller than the respective acoustic wave-lengths.

The experiments were carried out in the viscous forces domain with respect to the inertial forces, at a constant Reynolds number $Re=0.24$, in an emerging Oseen regime with very weak asymmetries in the flow field. For the first time this paper presents a complete collection of particle interactions at acoustic entrainments varying from $q_p$=0.84 to $q_p$ =0.05, i.e., covering practically its complete range of variability.

It is experimentally confirmed for the first time the presence of the mutual radiation pressure as a disturbing effect on the acoustic agglomeration generated on the aerosols, that is produced by the acoustic wake effect. Our results coincide with other previous researchs, agreeing with the theoretical prediction.

## INTRODUCTION

Since the sixties some small-scale experimental investigations were carried out on dilute aerosols to analyse acoustic agglomeration processes in them [1-5]. The observation of acoustic interactions between particles initially separated at distances much larger than their respective acoustic displacements, as well as the agglomeration found in monodisperse aerosols revealed the existence of hydrodynamic mechanisms generating the particle attractions through their sorrounding fluid. Most of these researchers observed in their experiments carried out with monodisperse aerosols the formation of pseudo-aggregation of oscillating aerosol particles, that brought together but remained separated at a certain distance without contact. This behaviour was attributed to contrary balanced hydrodynamic mechanisms of interaction. However, Hoffmann and Koopmann observed in 1996 particle collisions in monodisperse aerosols at acoustic frequencies over 700Hz [4]. They confirmed the presence of a hydrodynamic mechanism known as acoustic wake effect, causing attractions between particles aligned along the acoustic axis. In posterior experiments carried out by González *et al.*

(1997) with similar aerosols subjected to standing plane waves at a higher frequency (3kHz) [5], no pseudo-agglomerates were observed. On the contrary, attraction processes with particle collisions were found in the experiments.

The discrepancy of results between all these experiments demanded a clarification. With this aim, our paper presents an experimental research to analyse the influence exerted by the acoustic entrainment of single particles (acoustically oscillating) on their interaction processes and, in particular, on the hydrodynamic mechanisms that govern them.

While direct collisions produced between particles differently entrained by the acoustic field refer to the well known orthokinetic mechanism [6,7], other more complex processes of interaction are due to the hydrodynamic mechanisms. They generate particle attractions from larger distances of separation than their respective acoustic displacements. These mechanisms are related either to viscous asymmetries in the flow field around the particles, giving rise to the acoustic wake effect (AWE), and/or to nonlinear interactions produced between the particle scattered waves and the incident wave, known as mutual radiation pressure effect (MRPE). The influence of the particle entrainment coefficient on both hydrodynamic mechanisms is very complex and it has not been described up to now. The AWE generates a maximal attraction between particles aligned along the acoustic axis and becomes weaker at higher angles of their center-line with respect to that axis. Such an effect becomes intensified with a decrease of the particle entrainment factor [8]. On the contrary, the MRPE generates a maximal repulsion between particles aligned along the acoustic axis and a maximal attraction between particles perpendicularly orientated with respect to it.

**EXPERIMENTS**

More than 100 filmed interaction patterns were quantified and analysed in our experiments. Glass spheres with certified diameters of *8.0±0.9mm* immersed in air as very dilute aerosols (with a concentration smaller than 0.01%) were subjected to homogeneous plane standing waves with a constant velocity amplitude $U_0$=0.44m/s at diverse frequencies, ranging from 200Hz (at which the maximal entrainment factor of 0.86 was determined) up to 5kHz (at which the particles were less than 6% entrained by the acoustic field). The experiments were carried out at a constant Reynolds number *Re=0.24*, in an emerging Oseen regime.

A scheme of the employed experimental setup is shown in Figure 1. It consists of four parts: an acoustic cavity in which the particles are subjected to the acoustic field, an illumination system, a particle feeding device and an detection setup to visualize and process the images.

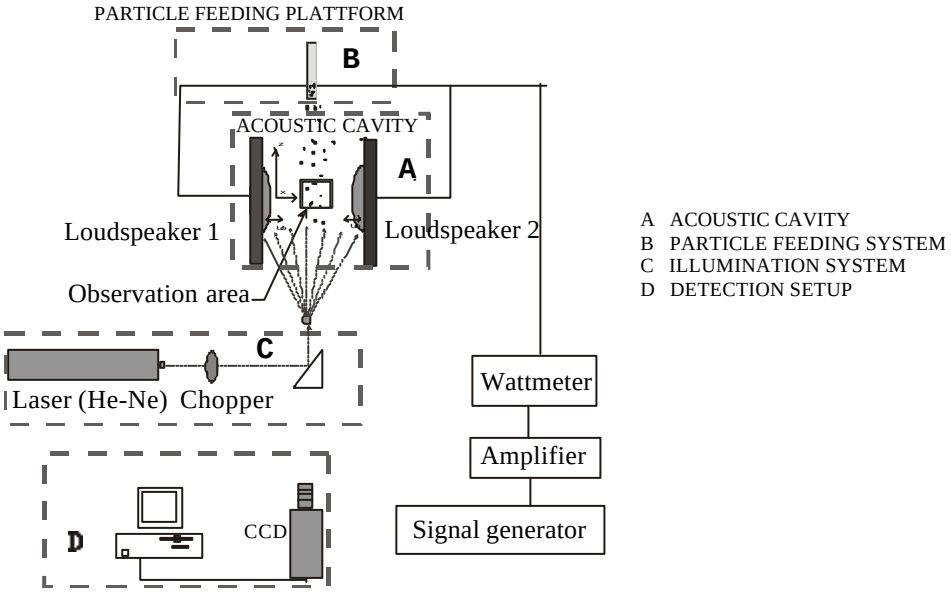


Figure 1: *Scheme of the setup*

The acoustic cavity consisted of two facing loudspeakers separated a distance *d* much smaller than one-half acoustic wavelength, where a horizontal homogeneous standing plane wave was established. The set-up for the optical image acquisition consisted of a CCD camera provided with a system of optical lenses and connected to a computer where the images were stored and processed. The optical resolution of the digitized images was variable and reached up to *2.94mm* per squared pixel. The particles, dropping in the gravitational field, crossed the acoustic cavity from its upper edge and were laterally entrained by the horizontal acoustic wave. The combination of both fields generated the particle sinusoidal trajectories, that were filmed as bright traces. These trajectories during the particle approach processes were reconstructed from partial cuts of consecutive frames pasted into a new picture. The well adjustment found between the edges of the particle trajectories from subsequent frames (with a duration of 20ms) made negligible the gap of time of the CCD capture.

To mantain the Reynolds number at a fixed value of *Re=0.24*, the incident wave velocity amplitude of $U_0$*=0.44m/s* was kept constant at the different applied frequencies. To this purpose, the displacement amplitude of the loudspeakers, $\hat{x}_0$, was varied at each selected frequency to satisfy $U_0 = 2\pi f x_0$. From the filmed pictures the acoustic particle displacements $\hat{x}_p$ were measured and compared to those displacements of the loudspeaker membranes (see [9]). Once computed the particle entrainment coefficient for each particle of the filmed interaction processes, their trajectories were analysed from the measured initial conditions $r_0$ and $\theta_0$. The time required by the particles to collide, $t_{col}$, was also determined in these reconstructed processes.

Experimental Results

Several attraction patterns were quantified and analysed at diverse measured entrainment coefficients, ranging from 0.85 to less than 0.06 (at variable frequencies from *f=200Hz* to *f=5kHz*). No interactions were observed between particles entrained by the acoustic field more than 50%. However, several particle attraction processes were visualized and quantified below this value. All of the observed approach processes started from separation distances between the particles much larger than their respective acoustic displacements, revealing the hydrodynamic character of their governing mechanisms.

At a measured entrainment coefficient $q_p$=0.46, attraction processes with particle collision were repeatedly observed, as shown in Figure 2.a, reconstructed from two consecutive frames. The particles approach mutually from $r_0$*=227.62±4.93mm* (*»28 $f_p$)* and $\theta_0$=0º±3.5 and collide after 80ms. This and other tunning-fork shaped attraction patterns generated for this entrainment factor from very low orientation angles evidence the presence of the AWE as a governing attraction mechanism, as previously confirmed at higher Reynolds numbers [4,5].

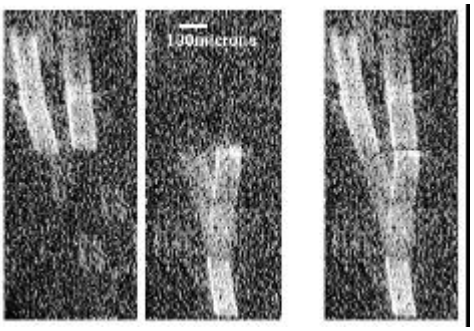

Figure 2.a: Reconstructed attraction pattern with particle collision for $q_p$=0.45

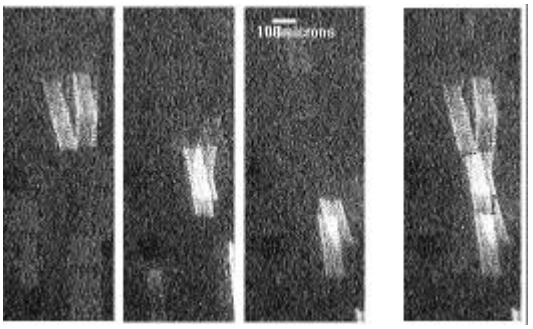

Figure 2.b: Reconstructed attraction pattern with particle divergence for $q_p$=0.45

However, the attraction processes found in our experiments at $q_p$*=0.46* do not always culminate in collision, as shown in Figure 2.b (from $r_0$*=160.10±4.93mm*(*»20 $f_p$)* and $\theta_0$=5.0±3.5º). After a time of approximately 34ms (24 acoustic cycles) the particles reach a maximal approaching

position without colliding and there start to diverge. This observation evidences the presence of combined opposite forces acting on the particles.

At a mesaured entrainment factor of $q_p$=0.35 attraction patterns culminating in particle collision were observed, as shown in Figure 3.a, where two particles initially aligned along the acoustic axis attract mutually from $r_0$=207.60±4.93mm(»20 $f_p$) and take a time 30ms to collide. However, a repulsion effect was detected at short distances of separation, as observed in Figure 3.b, where the particles started their attraction at $r_0$=134.40±4.93mm and $q_0$=15.2º±3.5º. After a time of approximately 30ms they reached their shortest distance of separation $r_1$=80±4.93mm (»10 $f_p$) from which on continued travelling in parallel without contact. It denotes once again the presence of balanced contrary forces acting on the particles.

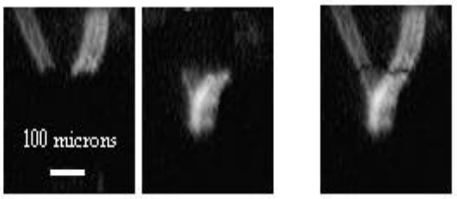


Figure 3.a: Reconstructed attraction pattern with particle collision for $q_p$=0.35

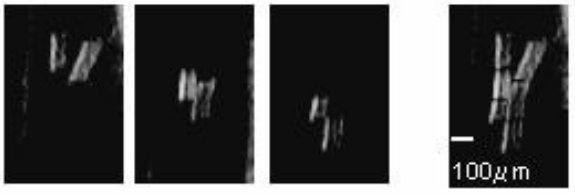


Figure 3.b: Reconstructed attraction pattern without particle collision for $q_p$=0.35

Combined approaching-divergent patterns were also filmed between pairs of particles at a measured entrainment coefficient $q_p$=0.25, as shown in the reconstructed pattern of Figure 4.a. The particles reach their shortest distance of $r_1$=41.0±4.93mm after approximately 30ms, and then the two hydrodynamic mechanisms become balanced. Nevertheless, attraction patterns with particle collision were also observed for this entrainment coefficient, as shown in Figure 4.b, started from $r_0$=98±4.93mm and $q_0$=36.5º±3.5º. In it a time of collision of app. 25ms was measured after a very elongated approach parabol.

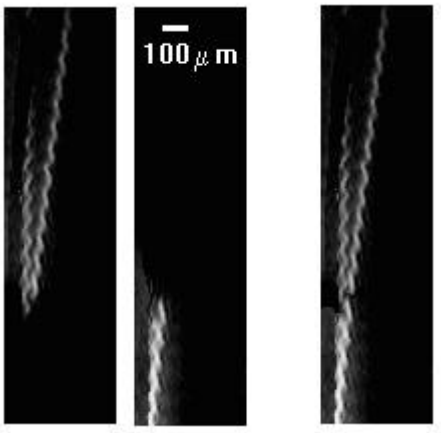


Figure 4.a: Reconstructed attraction pattern with particle collision for $q_p$=0.35

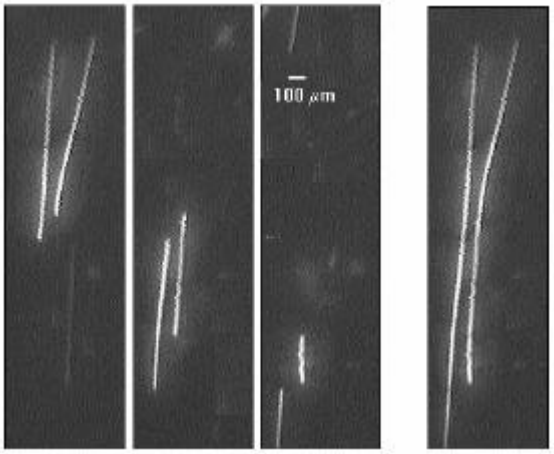


Figure 4.b: Reconstructed attraction pattern without particle collision for $q_p$=0.35

At entrainment factors lower than $q_p$=0.25, the particle displacements become smaller than the optical resolution of the digitized images. Hence their trajectories are observed as thick bright straight lines of 2-3 pixels (for a resolution of the digitized images of 4.93µm per pixel) instead of sinusoidal traces.

Below $q_p$=0.15 the observed attraction patterns started from angles up to 45º off the acoustic axis, evidencing again the negligible influence of the MRPE as an attraction mechanism. The process of Figure 5 was obtained at $q_p$=0.08. It started from $r_0$=190.08±5.94mm and $q_0$=-

*18.8º±3.5º* and required a time of $t_{col}$*=20ms* to reach the particle collision. At these low entrainment coefficients all the attraction processes were observed from angles up to 45º off the acoustic axis, evidencing again the negligible influence of the MRPE as an attraction mechanisms.


Figure 5: Reconstructed attraction process with particle collision for $q_p$=0.08

At the smallest measured value of $q_p$=0.05, the particles described very similar attraction behaviours. All the observed attraction patterns started from angles up to 45º off the acoustic axis and culminated in particle collision.
By reviewing the results obtained at diverse acoustic entrainments, a general decrease of the time of collision was found at lower entrainment coefficients. It can be observed in Table I if we compare those processes started from similar values of $r_0$ and $\theta_0$ but different values of $q_p$.

| $q_p$ | $r_0$ (µm) | $\theta_0$ | $t_{collision}$ (ms) |
|---|---|---|---|
| 0.46 | 212 | -20º | 40 |
| 0.46 | 142 | 0º | 33 |
| 0.46 | 259 | -23º | 40 |
| 0.46 | 229 | -30º | 34.32 |
| 0.40 | 162 | 11º | 25.72 |
| 0.40 | 165 | 40º | 40 |
| 0.35 | 141 | -43.6º | 40 |
| 0.35 | 207 | 0º | 30 |
| 0.30 | 212 | 0º | 20 |
| 0.30 | 147 | 13º | 25.72 |
| 0.30 | 234 | -24º | 40 |
| 0.30 | 130 | 23º | 20 |
| 0.30 | 202 | 12º | 20 |
| 0.30 | 127 | 8º | 20 |
| 0.25 | 211 | 0º | 20 |
| 0.25 | 134 | 36º | 28.57 |
| 0.25 | 98 | 36º | 18.59 |
| 0.25 | 155 | 12º | 17.16 |
| 0.25 | 202 | 0º | 20 |
| 0.20 | 148 | -35º | 20 |
| 0.20 | 193 | 0º | 20 |
| 0.20 | 280 | -8º | $30<t_{col}<40$ |
| 0.15 | 154 | -44º | $30<t_{col}<40$ |
| 0.15 | 123 | -18º | 20 |
| 0.15 | 209 | 8º | 40 |
| 0.15 | 65 | -39º | 20 |
| 0.12 | 138 | -34.56º | $40>t_{col}>20$ |
| 0.12 | 104 | 24º | 40 |
| 0.12 | 113 | -48º | 40 |
| 0.12 | 102 | 0º | 20 |
| 0.08 | 109 | 0º | 30 |
| 0.08 | 79 | -23º | 18.59 |
| 0.08 | 89 | 6º | 25.72 |
| 0.08 | 94 | 0º | 20 |
| 0.05 | 103 | -12º | $t_{col}<20$ |
| 0.05 | 108 | 23º | $t_{col}<20$ |
| 0.05 | 92 | 45º | $t_{col}<20$ |

Table I: Quantified attraction processes with particle collision

## CONCLUSIONS

For the first time a complete collection of quantified particle interactions is presented at diverse entrainment coefficients, covering almost its whole range of variability. Through the experiments we found the acoustic wake effect as the dominant mechanism causing particle attractions from distances of separation much larger than their respective acoustic displacements for all the measured entrainment coefficients below $q_p$=0.5 (over which not any interaction process was observed). However, the mechanism of the MRPE was also observed in the experiments acting as a disturbing effect against the particle attractions. This repulsion force becomes intense at short distances of separation (of the order of some particle diameters), overcoming sometimes the particle attractions originally induced by the AWE at low angles of orientation.

This action of the MRPE shows in the experiments a dependence on the particle entrainment, being the most intense at the higher entrainment coefficients (at which the maximal distances of separation from which on the particles diverged were quantified). For $q_p$<0.15 the influence of this mechanism becomes negligible and the observed attraction processes culminated in particle collision.

We also observed an experimental enhancement of the acoustic wake effect with the decrease of the acoustic entrainment in our experiments by means of an enshortment of the times of collision. It confirms for the first time what was theoretically expected in previous papers [5,10].

In addition, our experimental results confirm those previously obtained by Buranov et al [1] and those of Hoffmann and Koopmann [5], that showed pairs of particles narrowly spaced without contact forming "pseudo-agglomerates" at entrainment coefficients higher than $q_p$=0.15. Our present results also confirm the last experimental results obtained by González et al. [5] at an entrainment factor $q_p$ =0.08, where complete approach processes with particle collision was found in more than 46 quantified attraction patterns.

## REFERENCES


[1] Buranov, L, Eknadiosyants, O. (1962) *On the behaviour of aerosol particles in an acoustic field*, Sov. Phys. Acoust. **7**, 4, pp:398-399.

[2] Shirokova, L, Eknadiosyants, O (1966) *Interaction of aerosol particles in an acoustic field*, Sov. Phys. Acoust. **11**, 3, pp:346-348.

[3] Temkin, S, Ecker, Z. (1989), *Droplet pair interactions in a shock-wave flow field*, J. Fluid. Mech., **202**, pp:467-497.

[4] Hoffmann, T.L., Koopmann, G.H. (1996), *Visualization of acoustic particle interaction and agglomeration: Theory and Experiments*, J. Acoust. Soc. Am., **99,** 4, pp:2130-2141.

[5] González, I., Hoffmann T.L., Gallego-Juárez, J.A. (2002), *Visualization of acoustic particle interactions: Validation of a numerical model*
ACUSTICA-ACTA ACUSTICA, **87**,6, pp:19-26.

[8] González, I., Hoffmann, T.L., Gallego-Juárez, J.A. (2000), *Theory and calculations of sound induced particle interactions of viscous origin,* ACUSTICA-ACTA ACUSTICA, **86**, pp: 784-797.

[9] González, I., Hoffmann, T.L, Gallego-Juárez, J.A. (2000), *Precise measurement of particle entrainments in a standing-wave acoustic field between 20Hz and 3.5kHz***,** J. Aerosol Sci, **31,** 12, pp:1461-1468.

[10] Dianov, D.B., Podolskii, A.A., Turubarov, V.I. (1968), *Calculation of the hydrodynamic interaction of aerosol particles in a sound field under Oseen flow conditions*, Soviet Phys. Acoust., **13**, 3, pp. 314-319.